

Transport and Lifetime Enhancement of Photoexcited Spins in GaAs by Surface Acoustic Waves

T. Sogawa,^{1,2} P. V. Santos,^{1,*} S. K. Zhang,¹ S. Eshlaghi,³ A. D. Wieck,³ and K. H. Ploog¹

¹Paul-Drude-Institut für Festkörperelektronik, Hausvogteiplatz 5–7, 10117 Berlin, Germany

²NTT Basic Research Laboratories, 3-1 Morinosato-Wakamiya, Atsugi, Kanagawa 243-0198, Japan

³Lehrstuhl für Angewandte Festkörperphysik, Ruhr-Universität Bochum, 44780 Bochum, Germany

(Received 23 March 2001; published 13 December 2001)

We demonstrate spin transport and spin lifetime enhancement in GaAs quantum wells induced by the traveling piezoelectric field of a surface acoustic wave (SAW). Spin transport lengths of about $3\ \mu\text{m}$ corresponding to spin relaxation times during transport over 1 ns are observed, which are considerably longer than the exciton spin diffusion lengths in the absence of a SAW. The slow spin relaxation is attributed to a reduced electron-hole exchange interaction, when the carriers are spatially separated by the lateral potential modulation induced by the SAW.

DOI: 10.1103/PhysRevLett.87.276601

PACS numbers: 72.25.Dc, 72.25.Rb, 77.65.Dq, 78.55.-m

In recent years, *spintronics* (or spin electronics), a field aimed at the control and manipulation of the spin degrees of freedom in semiconductors, has become an active research area. Spin manipulation of free carriers and, in particular, spin transport is one of the most important steps towards the realization of novel functional devices such as spin transistors and quantum computing components [1,2]. Electron spin transport under a dc electric field was studied in *n*-type bulk GaAs by Kikkawa and Awschalom [3], who demonstrated long spin transport lengths using Faraday-rotation experiments. Ohno *et al.* [4] employed electroluminescence to evidence hole-spin injection from a ferromagnetic *p*-type (Ga,Mn)As layer into an intrinsic (In,Ga)As quantum well (QW). The same group has recently demonstrated the active control of magnetic properties in diluted magnetic semiconductors by electric fields [5].

A challenge faced in the manipulation and transport of photogenerated spins in intrinsic semiconductor QW's is associated with the strong exchange interaction between electron and hole spins in electron-hole (*e-h*) pairs [6,7]. The different conduction and valence band edge states in III-V semiconductors lead, in the single electron picture, to different relaxation times for hole (τ_h) and electron spins (τ_e). Although the Coulomb interaction, which is responsible for exciton formation, does not directly couple the electron and hole spins, it increases the overlap between the electron and hole wave functions. The latter enhances the exchange interaction between the electron and hole spins, which then becomes a main relaxation mechanism for photoexcited spins with relaxation times comparable to or shorter than those expected from τ_h and τ_e [6–9]. The previous considerations suggest the possibility of controlling the lifetime of photogenerated spins in undoped QW's by spatially separating photoexcited electrons and holes, as has been demonstrated using an electric field in Ref. [8].

In this Letter, we demonstrate the transport and the enhancement of the lifetime of photoexcited spins in intrinsic GaAs QW's modulated by a surface acoustic wave (SAW). The spatially modulated piezoelectric field of a SAW pro-

vides an efficient way of separating and transporting photogenerated *e-h* pairs in QW's over macroscopic distances [10]. Carrier transport takes place through the ionization of photoexcited *e-h* pairs and subsequent trapping of the electrons and holes at the minima and maxima, respectively, of the moving piezoelectric field. The spatial carrier separation in the type-II-like potential modulation leads to a significant increase of the recombination lifetime [10–12]. We demonstrate here that also the spin lifetime of the carriers becomes considerably enhanced under a SAW, so that they can be transported over several micrometers while maintaining their spins. We attribute the spin lifetime enhancement to a reduction of the exchange interaction induced by the spatial separation of the *e-h* pairs.

The experiments were carried out on a sample containing several GaAs single QW's with short period (AlAs/GaAs) superlattice barriers grown by molecular beam epitaxy on (001) GaAs [13]. We report results obtained on two QW's with thicknesses of 19.8 nm (QW₁) and 15.4 nm (QW₂) located 400 and 350 nm below the surface, respectively. SAW's propagating along the $[1\bar{1}0]$ surface direction were generated by interdigital transducers [(IDT's); cf. Fig. 1] designed for operation at a wavelength $\lambda_{\text{SAW}} = 5.6\ \mu\text{m}$ [corresponding to a frequency $\omega_{\text{SAW}}/(2\pi) = 520\ \text{MHz}$ at 16 K]. The SAW intensity will be expressed in terms of the nominal radio-frequency (rf) power P_{rf} (in dBm) applied to the transducer. rf coupling losses and attenuation of the SAW fields by carriers reduce the actual SAW acoustic power by $\Delta P_{\text{rf}} = 8$ to 12 dB as determined from rf transmission measurements.

The studies were performed using spin-resolved microphotoluminescence (μ -PL) spectroscopy to investigate the simultaneous transport of carriers and of spins by SAW's in GaAs QW's. A cw Ti:sapphire laser operating at 1.65 eV was used for PL excitation. This excitation energy lies above the electron-light hole (*e-lh*) transition of the QW's. The optical measurements were carried out at 16 K using a special μ -PL confocal microscope with illumination and detection areas each with a radius r of $\approx 2\ \mu\text{m}$.

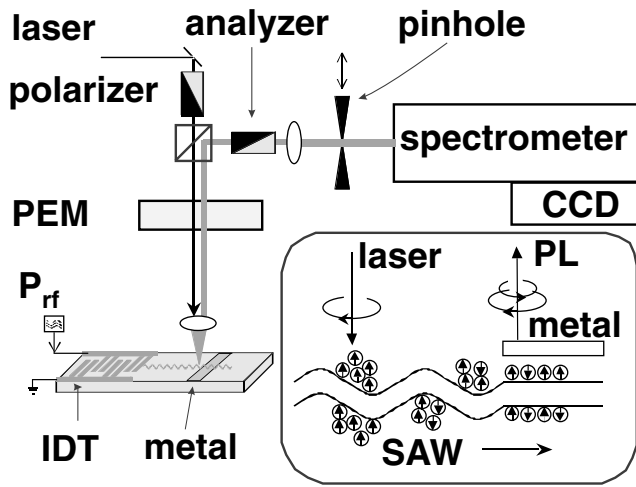


FIG. 1. Setup for spin sensitive μ -PL. Inset: for transport measurements, spin-polarized carriers generated by circularly polarized light (long \downarrow arrow) are detected at a second position by analyzing the circular PL polarization (long \uparrow arrow).

Spin sensitivity was achieved by including a photoelastic modulator (PEM) and polarization elements (a polarizer and an analyzer) in the optical path. The periodic phase retardation $\delta(t) = \delta_0 \sin(\omega_m t)$ introduced by the PEM modulates the generation rates of up (G_\uparrow) and down (G_\downarrow) spins at the PEM oscillation frequency $\omega_m = 50$ kHz. This frequency is low enough for the carriers to follow adiabatically the modulation changes. The angular position of the polarizer and analyzer were set to $+45^\circ$ and -45° with respect to the optical axis of the PEM. The latter was oriented along one of the samples $\langle 110 \rangle$ surface directions in order to avoid contributions from the SAW-induced linear birefringence [14].

Under the described conditions, the setup in Fig. 1 becomes a sensitive polarization bridge for optical orientation experiments. Its operation can be easily understood if we consider the particular time when $\delta(t) = \pi/4$, so that the input light becomes circularly polarized after passing through the PEM. If the optically oriented photogenerated carriers maintain their spins until recombination (i.e., when their spin lifetime τ_s is long compared with the radiative recombination lifetime τ_r), the electron-heavy hole (e -hh) PL of intensity I_0 will have the same circular polarization as the incident light. After the second pass through the PEM, the emitted light will emerge with a linear polarization parallel to the analyzer transmission axis. The signal detected by the charge-coupled device (CCD) will then be $I_{\text{CCD}}^{\text{ON}} = I_0$. In contrast, if the PEM retardation is set to zero, the PL will have no preferential orientation (provided that the spin coherence time is much smaller than the recombination lifetime). The detected intensity then becomes $I_{\text{PL}} = I_{\text{CCD}}^{\text{OFF}} = I_0/2$. The same intensity would be measured, if the carriers completely lose their spin memory before recombination, leading to a depolarized PL. The relative degree of spin polarization is then proportional to $\Delta I_{\text{PL}}/I_{\text{PL}}$, where $\Delta I_{\text{PL}} = I_{\text{CCD}}^{\text{ON}} - I_{\text{CCD}}^{\text{OFF}}$.

In order to account for finite spin relaxation times, we neglect dark exciton states ($|\pm 2\rangle$) [9]. The densities of up (n_\uparrow) and down (n_\downarrow) photoexcited spins are then given by

$$\frac{dn_{\uparrow(\downarrow)}}{dt} = -\frac{n_{\uparrow(\downarrow)}}{\tau_r} - \frac{n_{\uparrow(\downarrow)} - n_{\downarrow(\uparrow)}}{\tau_s} + G_{\uparrow(\downarrow)}. \quad (1)$$

The time-averaged degree of spin polarization $\rho = \frac{n_\uparrow - n_\downarrow}{n_\uparrow + n_\downarrow}$ becomes

$$\rho = \frac{\tau_{\text{eff}}}{\tau_r} \rho_0 = \frac{2}{1 - J_0(2\delta_0)} \frac{\Delta I_{\text{PL}}}{I_{\text{PL}}}, \quad (2)$$

where $\tau_{\text{eff}}^{-1} = \tau_r^{-1} + 2\tau_s^{-1}$ defines the inverse relaxation time of the net spin density ($n_\uparrow - n_\downarrow$) [15]. The initial degree of spin polarization after optical orientation ρ_0 depends on the PL excitation energy. In the data analysis, we used $\rho_0 = 0.5$, which corresponds to the expected value for excitation above the e -lh transition of the QW's [16]. The Bessel function J_0 accounts for the time dependence of the PEM retardation. In order to maximize the detected signal, the experiments were carried out using a retardation $\delta_0 = 1.9$ rad.

Typical excitonic e -hh PL (I_{PL} , lines) and polarization difference spectra (ΔI_{PL} , dots) measured for coincident positions of the illumination and detection spots are displayed in Fig. 2. Under low rf powers [Fig. 2(a)], the (e -hh) lines at 1.5284 and 1.5362 eV for QW₁ and QW₂, respectively, have widths less than 0.6 meV. For high SAW intensities [cf. Fig. 2(b)], each line splits into two due to the band gap modulation induced by the strain field of the SAW [14]. Note that the spin polarization ratio ρ is substantially larger in Fig. 2(b).

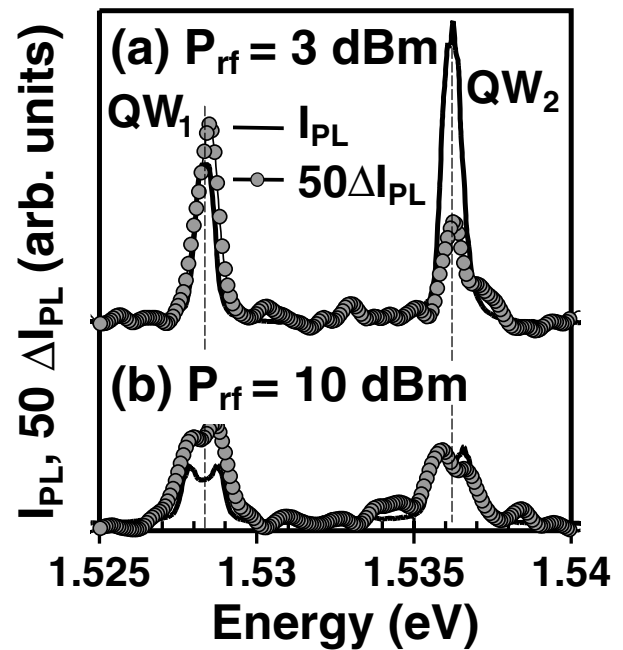


FIG. 2. Photoluminescence (I_{PL} , lines) and polarization difference signal ΔI_{PL} (dots) for different rf excitation powers.

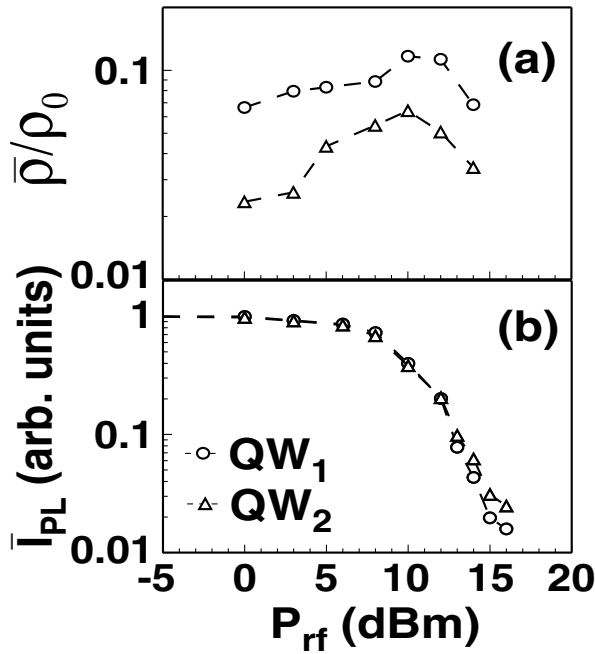


FIG. 3. (a) Average degree of spin polarization $\bar{\rho}$ and (b) integrated PL intensity (\bar{I}_{PL}) as a function of the nominal rf power applied to the IDT. \bar{I}_{PL} is normalized to the values measured without SAW.

The dependences of the energy-averaged degree of spin polarization ($\bar{\rho}$) and of the integrated PL intensity (\bar{I}_{PL}) are displayed in Figs. 3(a) and 3(b), respectively. $\bar{\rho}$ was obtained from the integrated intensities of \bar{I}_{PL} and $\Delta\bar{I}_{PL}$ using Eq. (2). For $P_{rf} > 8$ dBm, exciton ionization by the SAW piezoelectric field sets in; above 12 dBm the e - h pairs are completely ionized and transported out of the detection spot by the traveling potential, leading to a strong reduction in \bar{I}_{PL} . Since $\bar{\rho} < 0.1$ over the whole rf power range, $\tau_s \approx 2\tau_{eff} = 2\frac{\bar{\rho}}{\rho_0}\tau_r$. $\bar{\rho}$ and, consequently, τ_s show a substantial enhancement with increasing SAW amplitude for $P_{rf} < 10$ dBm. Interestingly, enhanced spin lifetimes are already observed for $P_{rf} < 8$ dBm, where no significant exciton ionization effects take place. τ_s reaches a maximum around $P_{rf} = 10$ dBm and reduces for powers above 12 dBm.

Spin transport was measured by detecting the PL polarization from spin-polarized carriers generated at a distant spot, as shown in the inset in Fig. 1. The separation between generation and recombination spots was achieved by shifting the pinhole in Fig. 1 from the confocal position. In order to increase the PL intensity, the detection position was placed close to the edge of a thin stripe of semitransparent nickel-chromium film. Since the QW's are located close to the surface, the thin metal film effectively short-circuits the longitudinal component of the SAW piezoelectric field, thus forcing the recombination of the transported carriers [10].

The total density of transported carriers [$(n_1 + n_1) \propto \bar{I}_{PL}$, open symbols] and the net spin density [$(n_1 - n_1) \propto \Delta\bar{I}_{PL}$, filled symbols] for QW₁ (circles) and QW₂ (triangles)

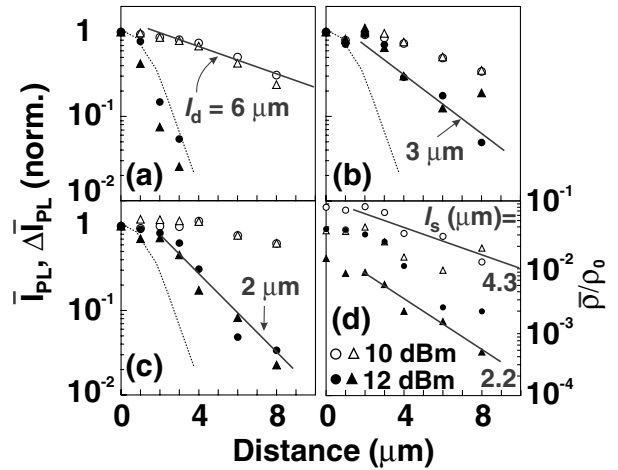


FIG. 4. Integrated PL [$\bar{I}_{PL} \propto (n_1 + n_1)$, open symbols] and PL polarization [$\Delta\bar{I}_{PL} \propto (n_1 - n_1)$, filled symbols] of QW₁ (circles) and QW₂ (triangles) for (a) no rf excitation, (b) $P_{rf} = 10$ dBm, and (c) $P_{rf} = 12$ dBm. (d) Spatial dependence of the degree of spin polarization $\bar{\rho}$. The dotted lines display the laser reflection profile. The characteristic decay lengths were obtained from exponential fits (lines) to the data.

gles) are plotted in Figs. 4(a) to 4(c) in the absence of rf excitation and for rf powers $P_{rf} = 10$ dBm and 12 dBm, respectively, as a function of the distance d between the generation and detection spots. The data are normalized to the values for $d = 0$. The dotted line shows the reflection profile of the excitation laser, which yields the spatial resolution $r = 2 \mu\text{m}$ of the optical setup. In the absence of a SAW, the PL profiles display an exponential decay for distances large compared with the radius r of the illumination spot [straight line in Fig. 4(a)]. Such behavior is expected for diffusion in two dimensions: from the decay length, we calculate comparable exciton diffusion lengths $l_d \approx 6 \mu\text{m}$ for both QW's. Under a SAW, the PL maxima shift along the SAW propagation direction, thus evidencing the transport of e - h pairs by the traveling SAW piezoelectric field [10]. The carrier transport distance increases with increasing SAW intensity. Note that the decay of \bar{I}_{PL} under a SAW is partially due to carrier diffusion in the direction perpendicular to the SAW propagation path, which leads to a reduced recombination within the detection spot.

The net spin profiles in the absence of a SAW show decay lengths comparable to the half-width of the laser reflection profile [cf. Fig. 4(a)], thus indicating spin diffusion lengths below the experimental resolution. In contrast, spin transport over distances considerably larger than the experimental resolution is observed under a SAW [Figs. 4(b) and 4(c)]. The characteristic spin transport length, obtained from a single exponential fit to the data (straight lines), is about $3 \mu\text{m}$ for $P_{rf} = 10$ dBm and decreases to $2 \mu\text{m}$ for $P_{rf} = 12$ dBm.

The spatial dependence of the spin polarization $\bar{\rho}$ for different rf powers and QW widths is displayed in Fig. 4(d). The $\bar{\rho}$ values for $d = 0$ in this figure are lower (by a factor of ≈ 2) than those in Fig. 3(a). This is attributed to the

partial screening of the piezoelectric field close to the metal stripe, which leads to shorter spin lifetimes. The effective spin relaxation length during transport l_s , defined as the exponential decay length of $\bar{\rho}$, decreases from $4.3 \mu\text{m}$ at $P_{\text{rf}} = 10 \text{ dBm}$ to $2.2 \mu\text{m}$ at $P_{\text{rf}} = 12 \text{ dBm}$ [lines in Fig. 4(d)]. Since the SAW piezoelectric potential prevents carrier diffusion along the SAW propagation direction, the spin relaxation time during the transport process can be obtained from the ratio between the relaxation length l_s and the SAW propagation velocity of 2910 m/s in the QW samples. Spin relaxation times of roughly 1.5 and 0.8 ns are estimated for rf powers of 10 and 12 dBm , respectively. These values exceed the typical exciton spin relaxation times in intrinsic QW's by over an order of magnitude [9].

In order to discuss the results, we consider two different spin relaxation mechanisms [7]. The first is exciton spin relaxation, which is directly probed in the confocal PL measurements presented in Fig. 3. The exciton spin relaxation time τ_s^{ex} is expected to be dominated by the exchange contribution, which can be expressed as [6,7] $\tau_s^{\text{ex}} \propto \frac{1}{|\Omega|^2 \tau_{\text{ex}}^*}$. Here, $|\Omega|^2$ is the strength of the exchange term, proportional to the overlap between the electron and hole wave functions, and τ_{ex}^* denotes the exciton scattering time. The QW's used in the present studies have very small PL linewidths. The scattering times are expected to be very long, thus leading to the small spin polarization degrees for low rf powers. The increased exciton spin relaxation times under a weak SAW, which are observed [cf. Fig. 3(a)] in an intensity range where no appreciable exciton ionization takes place, are attributed to (i) the enhanced exciton scattering due to the SAW potential (see below) as well as to impact with accelerated carriers and (ii) the reduced overlap of the e - h wave function under the influence of the SAW piezoelectric field.

Large SAW intensities ionize the excitons, so that the spin relaxation times probed in transport experiments (cf. Fig. 4) are mainly related to those of single electrons (τ_e) and holes (τ_h). For the nonresonant excitation used (with densities $>10^9$ carriers/cm²), the hole spin is expected to flip much faster than that of the electrons [7,9,17]; the polarization of the PL will basically depend on τ_e . In intrinsic samples, the latter is dominated by the D'yakonov-Perel [16] (DP) mechanism, associated with the spin splitting of the conduction band, and by the Elliot-Yafet (EY) mechanism [18], which results from a combination of the spin-orbit coupling with electron scattering. The τ_e 's predicted by these mechanisms are normally much longer than those from the exchange interaction, thus explaining the long spin relaxation times during transport.

Finally, the data in Fig. 4 indicate a reduction in spin lifetime for SAW powers exceeding 10 dBm . This reduc-

tion is probably associated with additional channels for the DP and EY processes under the SAW fields [19]. We have recently reported on the hh-lh mixing due to the strain field induced by a SAW [14], which becomes particularly strong for P_{rf} beyond 10 dBm . The spin relaxation time determined by the EY mechanism should be proportional to the carrier scattering time τ_c , while that from the DP mechanism should be inversely proportional to τ_c . The reduction of τ_c with SAW intensities for large rf powers seems, therefore, to favor the EY mechanism. Further experiments are under way to clarify these effects.

In conclusion, investigations of microscopic exciton and spin transport induced by SAW's in GaAs QW's demonstrate spin transport over distances exceeding $3 \mu\text{m}$. The corresponding spin relaxation times of a few ns are up to 2 orders of magnitude longer than in the absence of a SAW. The long spin relaxation is attributed to the reduction of the exciton exchange interaction, as electrons and holes are spatially separated by the lateral potential modulation induced by the SAW. The results thus demonstrate the control of exciton spin lifetime and of spin transport by a SAW in intrinsic semiconductors.

We thank H. Grahn for comments and for a critical reading of the manuscript. Support from the Deutsche Forschungsgemeinschaft (Projects No. SA598/2-1, No. GRK384, and No. SFB491) is also acknowledged.

*Email address: santos@pdi-berlin.de

- [1] G. A. Prinz, *Phys. Today* **48**, No. 4, 58 (1995).
- [2] C. H. W. Barnes, J. M. Shilton, and A. M. Robinson, *Phys. Rev. B* **62**, 8410 (2000).
- [3] J. M. Kikkawa and D. D. Awschalom, *Phys. Rev. Lett.* **80**, 4313 (1998).
- [4] H. Ohno *et al.*, *Nature (London)* **402**, 790 (1999).
- [5] H. Ohno *et al.*, *Nature (London)* **408**, 944 (2000).
- [6] M. Z. Maialle, E. A. de Andrada e Silva, and L. J. Sham, *Phys. Rev. B* **47**, 15 776 (1993).
- [7] L. J. Sham, *J. Phys. Condens. Matter* **5**, A51 (1993).
- [8] A. Vinattieri *et al.*, *Appl. Phys. Lett.* **63**, 3164 (1993).
- [9] L. Munöz *et al.*, *Phys. Rev. B* **51**, 4247 (1995).
- [10] C. Rocke *et al.*, *Phys. Rev. Lett.* **78**, 4099 (1997).
- [11] K. S. Zhuravlev *et al.*, *Appl. Phys. Lett.* **70**, 3389 (1997).
- [12] P. V. Santos, M. Ramsteiner, and F. Jungnickel, *Appl. Phys. Lett.* **72**, 2099 (1998).
- [13] S. Eshlaghi *et al.*, *J. Appl. Phys.* **86**, 6605 (1999).
- [14] T. Sogawa *et al.*, *Phys. Rev. B* **63**, 121307 (2001).
- [15] Ph. Roussignol *et al.*, *Surf. Sci.* **305**, 263 (1994).
- [16] M. I. D'yakonov and V. I. Perel, *Sov. Phys. JETP* **33**, 1053 (1971).
- [17] B. Baylac *et al.*, *Solid State Commun.* **93**, 57 (1994).
- [18] R. J. Elliot, *Phys. Rev.* **96**, 266 (1954).
- [19] V. K. Kalevich and V. L. Korenev, *JETP Lett.* **52**, 232 (1990).